

# Hydrogen peroxide mediates the radiation-induced mutator phenotype in mammalian cells

Disha DAYAL\*, Sean M. MARTIN\*, Charles L. LIMOLI† and Douglas R. SPITZ\*<sup>1</sup>

\*Free Radical and Radiation Biology Program, Department of Radiation Oncology, Holden Comprehensive Centre, The University of Iowa, Iowa City, IA 52242, U.S.A., and †Department of Radiation Oncology, The University of California, Irvine, CA 92697, U.S.A.

Chronic oxidative stress has been associated with genomic instability following exposure to ionizing radiation. However, results showing direct causal linkages between specific ROS (reactive oxygen species) and the ionizing radiation-induced mutator phenotype are lacking. The present study demonstrates that ionizing radiation-induced genomically unstable cells (characterized by chromosomal instability and an increase in mutation and gene amplification frequencies) show a 3-fold increase in steady-state levels of hydrogen peroxide, but not superoxide. Furthermore, stable clones isolated from parallel studies showed significant increases in catalase and GPx (glutathione peroxidase) activity. Treatment of unstable cells with PEG-CAT (polyethylene

glycol-conjugated catalase) reduced the mutation frequency and mutation rate in a dose-dependent fashion. In addition, inhibiting catalase activity in the stable clones using AT (3-aminotriazole) increased mutation frequency and rate. These results clearly demonstrate the causal relationship between chronic oxidative stress mediated by hydrogen peroxide and the mutator phenotype that persists for many generations following exposure of mammalian cells to ionizing radiation.

**Key words:** catalase, genomic instability, ionizing radiation, mutation rate, oxidative stress.

## INTRODUCTION

For many years, it was thought that genetic changes caused by radiation were only due to DNA damage derived from the incident free radical species produced at the time of exposure. However, it was discovered that the number of surviving cells exhibiting increased delayed mutation frequencies following ionizing radiation is greater than would be predicted if only the cells exposed at the time of irradiation were involved [1,2]. In other words, the mutagenic effects of ionizing radiation were found to be trans-generational. These persistent trans-generational mutagenic effects, apparently resulting from a mutator phenotype, have collectively been called non-targeted or bystander effects of radiation, but the mechanisms governing these phenomena are not well understood [1,2].

Chronic oxidative stress mediated by continuous exposure to H<sub>2</sub>O<sub>2</sub> or 95% O<sub>2</sub> has been shown to induce genomic instability and gene amplification in hamster fibroblasts [3]. Additional studies investigating the cause of ionizing radiation-induced genomic instability have suggested that persistent metabolic oxidative stress may be involved [4,5]. Hydroperoxides produced by metabolic processes have been suggested to contribute to persistent ionizing radiation-induced genomic instability [6,7] on the basis of data gathered using non-specific oxidation-sensitive probes. However, direct causal linkages between increased steady-state levels of specific ROS (reactive oxygen species), such as H<sub>2</sub>O<sub>2</sub>, and the mutator phenotype characterized by increased rates of delayed mutagenesis following exposure to ionizing radiation are lacking.

In the present study, three subsets of Chinese hamster ovary fibroblasts (GM10115 cells) were used to determine the involve-

ment of H<sub>2</sub>O<sub>2</sub> in the ionizing radiation-induced mutator phenotype: (i) the untreated parental GM10115 cell line, (ii) unstable GM10115 clones designated CS-9 and LS-12, and (iii) stable clones designated 114 and 118 [8]. We now show that the unstable clones not only exhibit increased mutation frequency and rates, but were also found to produce greater steady-state levels of H<sub>2</sub>O<sub>2</sub> relative to the parental cell line and stable clones. The stable clones were found to have increased catalase and GPx (glutathione peroxidase) activities relative to the unstable clones. Furthermore, both increased mutation frequency and increased mutation rates in the unstable clones were suppressed by a cell-permeant H<sub>2</sub>O<sub>2</sub>-scavenging enzyme, PEG-CAT [PEG (polyethylene glycol)-conjugated catalase]. Mutation frequencies and rates could be increased in the stable clones treated with the catalase inhibitor AT (3-aminotriazole). These results provide unambiguous evidence showing that H<sub>2</sub>O<sub>2</sub> mediates the persistent mutator phenotype in these mammalian cells and suggest that scavengers of H<sub>2</sub>O<sub>2</sub> could be used to inhibit chronic indications of genomic instability persisting many generations after exposure to a range of cytotoxic treatments.

## MATERIALS AND METHODS

### Cell culture

The Chinese hamster ovary parental cell line GM10115 was obtained from A.T.C.C. Cell stock flasks were grown in DMEM (Dulbecco's modified Eagle's medium) with high glucose and 1 mM sodium pyruvate (CellGrow), 10% fetal bovine serum (Hyclone), 0.2 mM L-proline and 1% L-glutamine (Gibco). The

Abbreviations used: AT, 3-aminotriazole; CAD, carbamoyl-*P* synthetase/aspartate transcarbamylase/dihydro-orotase; DHE, dihydroethidium; c-DCF, 5-(and 6)-carboxy-2'-7'-dichlorofluorescein; c-DCFH<sub>2</sub>, 5-(and 6)-carboxy-2',7'-dichlorodihydrofluorescein diacetate; DMPO, 5,5-dimethyl-1-pyrroline *N*-oxide; GPx, glutathione peroxidase; HAT, hypoxanthine/aminopterin/thymidine; HBSS, Hanks balanced saline solution; hprt, hypoxanthine-guanine phosphoribosyltransferase; NBT, Nitro Blue Tetrazolium; PALA, *N*-(phosphonoacetyl)-L-aspartate; PEG, polyethylene glycol; PEG-CAT, PEG-conjugated catalase; p-HPA, *p*-hydroxyphenylacetic acid; ROS, reactive oxygen species; SOD, superoxide dismutase.

<sup>1</sup> To whom correspondence should be addressed (email douglas-spitz@uiowa.edu)

previously described [8] stable (114, 118) and unstable (CS-9, LS-12) clones were grown in the same media.

### Mutation frequency assay

Cells ( $3 \times 10^6$ ) from an exponentially growing culture were seeded on to 100-mm-diameter dishes. DMSO was used to dissolve 6-thioguanine (Sigma) before it was added at a final concentration of  $40 \mu\text{M}$ . The dishes were left undisturbed for 2–3 weeks until colonies with at least 50 cells appeared. The colonies were then fixed, stained and counted. The data were normalized to plating efficiency of identically treated cells in the absence of 6-thioguanine.

### CAD (carbamoyl-*P* synthetase/aspartate transcarbamylase/dihydro-orotase) gene amplification assay

Amplification at the CAD gene locus was determined by plating  $3.5 \times 10^5$  cells on a 100-mm-diameter dish. Medium containing  $100 \mu\text{M}$  PALA (*N*-phosphonoacetyl-L-aspartate) [Developmental Therapeutics Program, NCI (National Cancer Institute)/NIH (National Institutes of Health)] was added and dishes were placed in a  $37^\circ\text{C}$  incubator for 2 weeks. The colonies were then fixed, stained and counted. The number of colonies was normalized to the plating efficiency.

### Oxidation of c-DCFH<sub>2</sub> [5-(and-6)-carboxy-2',7'-dichlorodihydrofluorescein diacetate] as an indicator of steady-state levels of pro-oxidants

Cells ( $3.5 \times 10^5$ ) were seeded on a 60-mm-diameter dish in complete medium (three replicates for each clone) and grown for 2 days. On day 2, the cells were washed with PBS, following which 2 ml of PBS was added to each dish and the dishes were incubated with  $10 \mu\text{g/ml}$  c-DCFH<sub>2</sub> (Invitrogen), or the oxidation-insensitive analogue c-DCF [5-(and 6)-carboxy-2'-7'-dichlorofluorescein], for 15 min at  $37^\circ\text{C}$ . The cells were then washed, trypsinized and centrifuged at  $400 g$  for 5 min. The pellet was resuspended in  $500 \mu\text{l}$  of PBS and filtered through a mesh to remove large aggregates. Live cells (10000; gated on forward and side scatter) were analysed for C-DCF fluorescence (FL1 channel,  $\lambda_{\text{excitation}} = 488 \text{ nm}$ ,  $\lambda_{\text{emission}} = 530 \text{ nm}$ , 30 nm bandpass) using a Beckton Dickinson FACScan. DMSO (0.1% v/v) and antimycin A ( $10 \mu\text{M}$ ) dissolved in DMSO were used as negative and positive controls respectively. CellQuest Pro software was used for data analysis.

### Oxidation of DHE (dihydroethidium) as an indicator of steady-state levels of superoxide

Cells ( $3.5 \times 10^5$ ) were seeded on 60-mm-diameter dishes (three replicates for each clone) and grown for 2 days in complete media. The cells were labelled, after washing the plates with PBS, by incubating at  $37^\circ\text{C}$  for 40 min with  $10 \mu\text{M}$  DHE (Invitrogen) and DMSO (0.1% v/v) in 2 ml PBS containing 5 mM pyruvate. The cells were then washed, trypsinized and centrifuged at  $400 g$  for 5 min. The pellet was resuspended in  $500 \mu\text{l}$  of PBS and filtered through a mesh to remove large aggregates. Live cells (10000), gated on forward and side scatter, were analysed for DHE fluorescence using a Beckton Dickinson FACScan (FL2 channel,  $\lambda_{\text{excitation}} = 488 \text{ nm}$ ,  $\lambda_{\text{emission}} = 585 \text{ nm}$ , 30 nm bandpass). DMSO (0.1% v/v) and antimycin A ( $10 \mu\text{M}$ ) dissolved in DMSO were used as negative and positive controls, respectively. CellQuest Pro software was used for data analysis.

### Extracellular hydrogen peroxide

The hydrogen peroxide assay was carried out as previously described [9]. Exponentially growing cells were washed with Phenol Red-free HBSS (Hanks balanced saline solution) three times. This was followed by the addition of glucose (final concentration 6.2 mM), Hepes (final concentration 1.0 mM), sodium bicarbonate (final concentration 6.0 mM), p-HPA (*p*-hydroxyphenylacetic acid, Sigma) (final concentration 1.6 mM) and HRP (horseradish peroxidase; final concentration  $95 \mu\text{g/ml}$ ). HBSS was used to bring the final volume to 1 ml. The cells were incubated at  $37^\circ\text{C}$  for 30 min, during which time H<sub>2</sub>O<sub>2</sub> accumulated in the extracellular medium. In the case of catalase samples, to verify that the signal was coming from H<sub>2</sub>O<sub>2</sub>, the dishes were incubated with catalase (1000 units) for 30 min prior to the addition of reaction mixture. The media was collected in a cuvette and the release of H<sub>2</sub>O<sub>2</sub> was followed fluorometrically (Perkin Elmer LS50B) by measuring the p-HPA dimer formed at excitation and emission wavelengths of 320 and 408 nm respectively. Quantitation was accomplished using comparison to a standard curve obtained from genuine H<sub>2</sub>O<sub>2</sub>. The pH of the samples was checked following incubation and did not change significantly.

### Isolation of mitochondria

Mitochondria were isolated from cells using density gradient centrifugation with a sucrose gradient in isolation buffer (0.25 M sucrose, 5 mM Hepes, 0.1 mM EDTA, pH 7.25) [10]. Exponentially-growing cells were harvested and centrifuged at  $500 g$ . The pellet was resuspended in isolation buffer and homogenized using a Dounce homogenizer rinsed with dilute HCl followed by distilled water. Cell debris was separated by centrifugation at  $1000 g$  for 10 min. The supernatant was collected from this step and centrifuged at  $10000 g$  for 10 min. The mitochondrial pellet was resuspended in  $500 \mu\text{l}$  of isolation buffer and used for further analysis. Protein was determined using the Bio-Rad protein assay protocol.

### EPR

EPR analysis was carried out on isolated mitochondria using a Bruker EMX spectrometer. Mitochondrial protein samples ( $100 \mu\text{g}$ ) were incubated with the DMPO (5,5-dimethyl-1-pyrroline *N*-oxide) spin trap (150 mM) for 2 min at room temperature ( $20\text{--}25^\circ\text{C}$ ). This was followed by a 10 min incubation with 9 mM succinate (pH adjusted to 7.4) at  $37^\circ\text{C}$ . To ascertain that the DMPO-OH EPR signal observed was indeed due to superoxide, CuZnSOD (Cu/Zn superoxide dismutase; 1000 units) was added 2 min prior to the addition of DMPO to suppress the EPR signal. The part of the signal that was suppressed by the enzyme was considered a true measure of superoxide and thus this portion was plotted. Spectra were collected using TM (transverse magnetic) cavity and a flat cell. Spectra were quantified by measuring the signal intensity of the two centre lines of DMPO-OH spectra ( $a^{\text{N}} = 14.9 G$  and  $a^{\text{H}} = 14.9 G$ ) and averaging these values [11]. The instrument parameters used were: sweep width 80 G, power 40 mW,  $\nu = 9.79 \text{ GHz}$ , scan rate 82 s, modulation amplitude 1 G, time constant 82 ms, number of scans = 10.

### GPx activity

To make cell homogenates, 50 mM potassium phosphate buffer (1:1 KH<sub>2</sub>PO<sub>4</sub>/K<sub>2</sub>PO<sub>4</sub>), pH 7.8, containing 1.34 mM DETAPAC (diethylenetriaminepenta-acetic acid), was added to cell pellets following one freeze/thaw cycle. GPx-1 activity was measured

using cumene hydroperoxide (Sigma) as the substrate by monitoring the disappearance of NADPH at 340 nm as described previously. Data were normalized per mg of protein as determined by the Lowry protein assay [12,13].

### Catalase assay

Catalase activity was determined by monitoring the disappearance of 10 mM H<sub>2</sub>O<sub>2</sub> in reactions containing cell homogenate as previously described [14]. Activity was expressed in mκ units/mg of protein.

### GSH measurements

The recycling assay of Anderson and Griffith [15,16] was used to determine glutathione content in cell homogenates and was normalized to protein content. GSSG was determined by incubating the sample with 2-vinylpyridine as previously described [16]. GSH and GSSG concentrations were reported in GSH equivalents using a standard curve.

### SOD activity assay

The SOD activity assay was performed as previously described [17]. Inhibition of NBT (Nitro Blue Tetrazolium) reduction was used as a marker of SOD activity. Samples were run either in the presence of 5 mM cyanide (for MnSOD activity) or in the absence of cyanide (for total SOD activity). MnSOD activity was subtracted from the total, and the propagation of errors theory was used to obtain CuZnSOD activity.

### PEG-CAT treatment

Exponentially growing cells ( $3 \times 10^6$ ) were seeded in 100 mm dishes, and 100 units/ml PEG-CAT (Sigma) (reconstituted in PBS) was added to each dish 2 h prior to the addition of 6-thioguanine. PEG was added at an equivalent concentration to the conjugated enzyme to control for any effects not specific to the enzyme activity.

### Aminotriazole treatment

Cells were grown in complete media with 20 mM AT for 4 days. On the fourth day, cells were trypsinized, counted, and  $3 \times 10^6$  cells were seeded in media containing 40 μM 6-thioguanine without AT. After 2 weeks, colonies were stained and counted. The effect of AT on the plating efficiency of cells was corrected for in the mutation frequency assay.

### Mutation rate assay

Cells were selected in media containing HAT (CellGrow) (hypoxanthine/aminopterin/thymidine) for 3 weeks. Following this, cells were grown in complete medium without HAT and mutation frequency was assayed immediately following removal from HAT selection (day 0) as well as after 10–15 days of passage in the absence of HAT. Mutation frequency was divided by the number of days out of selection to determine mutation rate/10<sup>6</sup> cells per day. The mutation rates for comparable groups were determined on the exact same day [18].

### Statistics

Statistics were performed using one-way ANOVA for non-parametric measurements. Tukey post-hoc test was performed wherever appropriate. Results were considered significantly different if  $P \leq 0.05$  unless otherwise mentioned. All statistical tests were done using GraphPad Prism software.

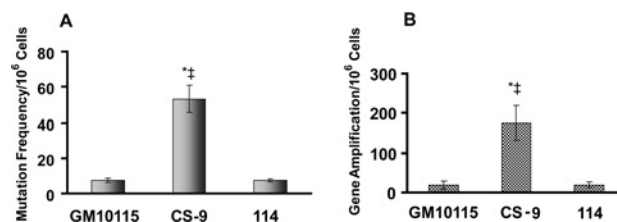


**Figure 1 CS-9 cells show increased genomic instability**

(A) To measure mutation frequency,  $3 \times 10^6$  cells were plated in 100-mm-diameter dishes containing complete medium and 40 μM 6-thioguanine. Dishes were left undisturbed in a 37°C incubator and colonies were counted after 2 weeks. Error bars represent  $\pm 1$  S.D. from five treatment dishes.  $P < 0.01$ ; \*against wild-type (GM10115), ‡against clone 114. (B) To measure CAD gene amplification,  $0.35 \times 10^6$  cells were plated on a 100-mm-diameter dish and media containing 100 μM PALA was added. Colonies were counted after 2 weeks. The error bars represent  $\pm 1$  S.D. from six dishes for GM10115 and clone CS-9, and three separate dishes for clone 114.  $P < 0.01$ ; \*against wild-type, ‡against clone 114.

## RESULTS

Clones used in this study were originally described by Limoli et al. [8]. Briefly, colonies derived from single cells surviving exposure to 10 Gy were expanded and analysed for multiple endpoints of genomic instability. To confirm past findings, and to verify that an unstable rather than a stable clone possessed a mutator phenotype, cells were analysed for mutation and gene amplification frequencies. Our data show that the unstable clone CS-9 exhibits higher (4- to 5-fold) mutation and gene amplification frequencies, at the *hprt* (hypoxanthine–guanine phosphoribosyltransferase) and CAD gene loci respectively, relative to the parental GM10115 and stable 114 clone (Figures 1A and 1B).

When steady-state levels of pro-oxidants were determined, the unstable clones (CS-9 and LS-12) demonstrated significantly increased c-DCFH<sub>2</sub> oxidation relative to the parental and the stable clone 114 (Figure 2A). These changes in c-DCFH<sub>2</sub> fluorescence were confirmed to be truly indicative of changes in steady-state pro-oxidant levels (and not changes in probe uptake, ester cleavage or efflux) because no significant changes in fluorescence were noted in co-cultures labelled with the oxidation-insensitive analogue, c-DCF (results not shown). Consistent with the c-DCFH<sub>2</sub> results, when a specific measure of extracellular H<sub>2</sub>O<sub>2</sub> production was determined (catalase-inhibitable p-HPA oxidation), the unstable clones (CS-9 and LS-12) were found to produce significantly more H<sub>2</sub>O<sub>2</sub> relative to the parental and stable 114 clone (Figure 2B). None of the unstable clones showed a consistent change in steady-state levels of superoxide in isolated mitochondria as determined by SOD-inhibitable EPR spectroscopy (Figure 2C), and only LS-12 showed a modest change in superoxide-sensitive DHE oxidation (Figure 2D). These results show that the unstable clones CS-9 and LS-12 appear to demonstrate increases in steady-state levels of H<sub>2</sub>O<sub>2</sub> relative to the parental and 114 stable clones. Interestingly, the stable 118 clone showed what appeared to be some increase in H<sub>2</sub>O<sub>2</sub> as well. However, since the intracellular redox status is also governed by antioxidant enzymes, the activities of primary antioxidant enzymes responsible for detoxification of superoxide (i.e. SOD) and hydrogen peroxide (i.e. GPx and catalase) were investigated.

Antioxidant enzyme analysis showed that the activities of the H<sub>2</sub>O<sub>2</sub>-scavenging enzymes catalase and GPx were significantly elevated in the stable clones 114 and 118 relative to the wild-type and unstable clones (Figure 3A). On the other hand, catalase and GPx activities in the unstable clones were either reduced or comparable with the wild-type. Since GPx activity is affected by

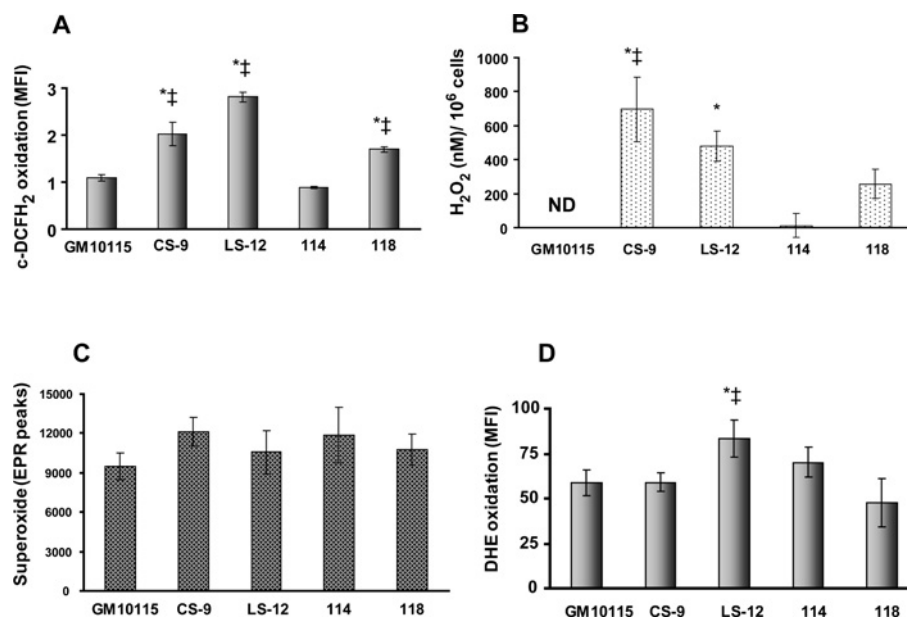


**Figure 2** Genomically unstable clones show increased steady-state levels of ROS

(A) Intracellular pro-oxidant status of cells was assessed using c-DCFH<sub>2</sub> staining. Cells were labelled with 10  $\mu$ g/ml c-DCFH<sub>2</sub> for 15 min at 37°C. Error bars represent  $\pm 1$  S.D. from three dishes.  $P < 0.05$ ; \*against wild-type, ‡against clone 114. (B) H<sub>2</sub>O<sub>2</sub> produced by cells was measured in the medium using the catalase-inhibitable p-HPA fluorescence. The error bars represent  $\pm$ S.E.M. of six dishes. ND stands for non-detectable.  $P < 0.05$ ; \*against wild-type, ‡against clone 114. (C) Superoxide was measured as the SOD-inhibitable DMPO-OH EPR signal from isolated mitochondria from each cell line. The error bars represent  $\pm$ S.E.M. from three independently-harvested samples. No statistical difference between cell lines was detected ( $P > 0.05$ ). (D) Estimation of intracellular superoxide using DHE oxidation. Cells were labelled with 10  $\mu$ M DHE at 37°C for 40 min. Error bars represent  $\pm 1$  S.D. of five dishes from each cell line.  $P < 0.05$ ; \*against wild-type, ‡against clone 118. MFI, mean fluorescence intensity.

the intracellular availability of reduced glutathione, glutathione levels were evaluated in these cell lines (Figure 3B). Consistent with increases in GPx activity, the stable clones had increases in GSH levels relative to the wild-type. It had been proposed that the product of intracellular GSH and GPx activity gives a more accurate reflection of “effective GPx activity” [19], which is a better indicator of the H<sub>2</sub>O<sub>2</sub>-detoxifying capacity of the cell. On doing this calculation and propagating the errors in both measurements, we observed that the effective GPx activity was elevated in both of the stable clones (Figure 3C). In addition, Figure 3(D) shows that there was no significant difference in either MnSOD or CuZnSOD activities in these clones. The results of the antioxidant enzyme analysis suggest that hydrogen peroxide removal may play a more critical role (as compared with superoxide removal) in governing radiation-induced genomic instability.

Together, these results suggest that increases in steady-state levels of H<sub>2</sub>O<sub>2</sub> may be causally related to radiation-induced genomic instability. To test this hypothesis, the mutation frequency assay was repeated in the presence of 100 units/ml PEG-CAT using the unstable CS-9 cells. Figure 4(A) demonstrates a dramatic suppression of mutation frequency in the PEG-CAT-treated CS-9 cells, which also showed a 2-fold increase in catalase activity relative to untreated cells. When the experiment was repeated using PEG alone, no suppression of mutation frequency was observed (results not shown), providing clear evidence for the role of catalase enzyme activity in the suppression of the mutator phenotype. Furthermore, PEG-CAT treatment demonstrated a dose–response relationship with suppression of mutation frequency (Figure 4B). To confirm further the causal role of H<sub>2</sub>O<sub>2</sub> in radiation-induced genomic instability, catalase activity was inhibited in the 114 stable clone using AT, and the 6-thioguanine mutation frequency assay was repeated. When

114 cells were grown in the presence of 20 mM AT for 4 days (85–90% inhibition of catalase activity) and then plated into 6-thioguanine for 2 weeks, mutation frequency was significantly increased 2–2.5-fold (Figure 4C).

Since the mutator phenotype induced following exposure to radiation is believed to be a dynamic self-perpetuating process, the next series of experiments were designed to determine mutation rates (as opposed to mutation frequency) in populations of genomically stable and unstable clones with or without manipulation of catalase activity. The cell populations were cleansed of pre-existing mutations at the *hprt* locus by passage in complete media supplemented with 1 $\times$ HAT for 3 weeks. Following HAT selection, cells were grown with or without manipulation of catalase activity for 10–15 days and then plated for the mutation frequency assay. Mutation frequency at a given time was divided by the number of days out of HAT selection to obtain the mutation rate. The results in Figure 4(D) show that the baseline mutation rate of the unstable clone (CS-9) was significantly higher than both wild-type (17-fold) and the stable clones (5- to 10-fold). Consistent with the hypothesis that H<sub>2</sub>O<sub>2</sub> is causally related to the radiation-induced mutator phenotype, treatment with 100 units/ml PEG-CAT completely suppressed the increased mutation rate demonstrated by CS-9. In addition, treatment of the stable clones 114 and 118 with the catalase inhibitor AT significantly increased mutation rates to a level greater than the wild-type. In fact, the AT-treated 118 clone demonstrated mutation rates similar to the CS-9 unstable clone (Figure 4D). Interestingly, the 114 clone, which had lower steady-state levels of H<sub>2</sub>O<sub>2</sub> (Figure 2B), demonstrated a smaller increase in mutation rate with AT treatment (Figure 4D) when compared with the stable clone 118, which had a higher baseline steady-state level of H<sub>2</sub>O<sub>2</sub> (Figures 2B and 4D) and showed a

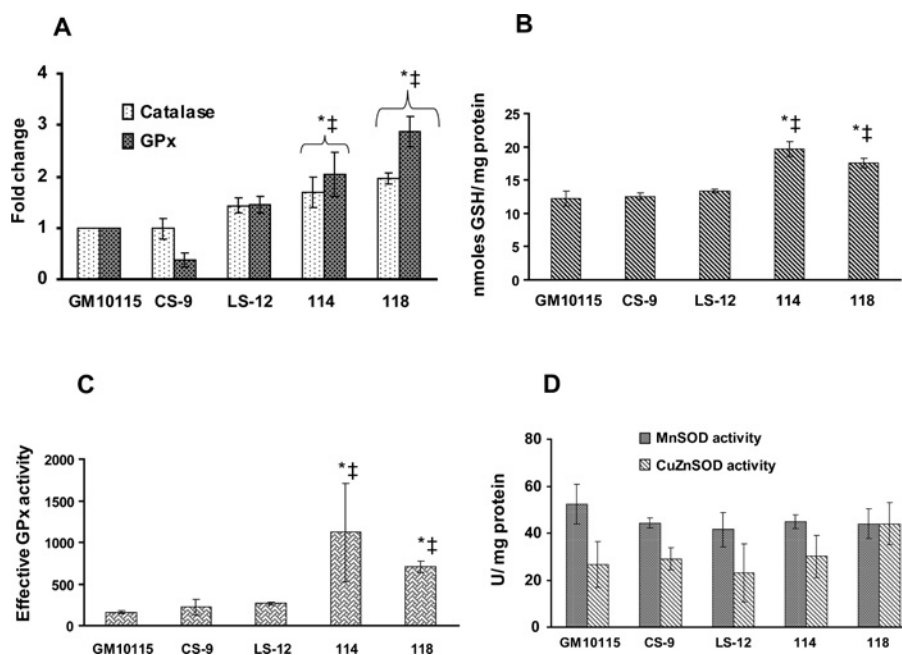


**Figure 3** Hydroperoxide-scavenging enzyme activity is increased in genomically stable clones

(A) GPx and catalase activities were analysed in cell homogenates and normalized to protein content. Data are represented as a fold change relative to wild-type (GM10115). The error bars for GPx activity represent  $\pm 1$  S.D. from four samples. The error bars for catalase activity represent  $\pm 1$  S.D. from three independently harvested samples from each group.  $P < 0.05$ ; \*against wild-type, ‡against clone CS-9. (B) GSH was measured using the DTNB [5,5'-dithiobis-(2-nitrobenzoic acid)] recycling assay. Error bars represent  $\pm 1$  S.D. from five samples.  $P < 0.05$ ; \*against GM10115, ‡against CS-9. (C) Using data in (A) and (B), effective GPx activity was calculated [19]. The errors in the GPx and GSH measurements were used to calculate the error for the effective GPx measurement using the propagation of error theory.  $P < 0.05$ ; \*against GM10115, ‡against clone CS-9. (D) CuZnSOD and MnSOD activities were measured in whole cell lysates using inhibition of NBT reduction as an indicator. Error bars represent  $\pm 1$  S.D. from four samples. No statistical differences were noted among the groups ( $P > 0.05$ ).

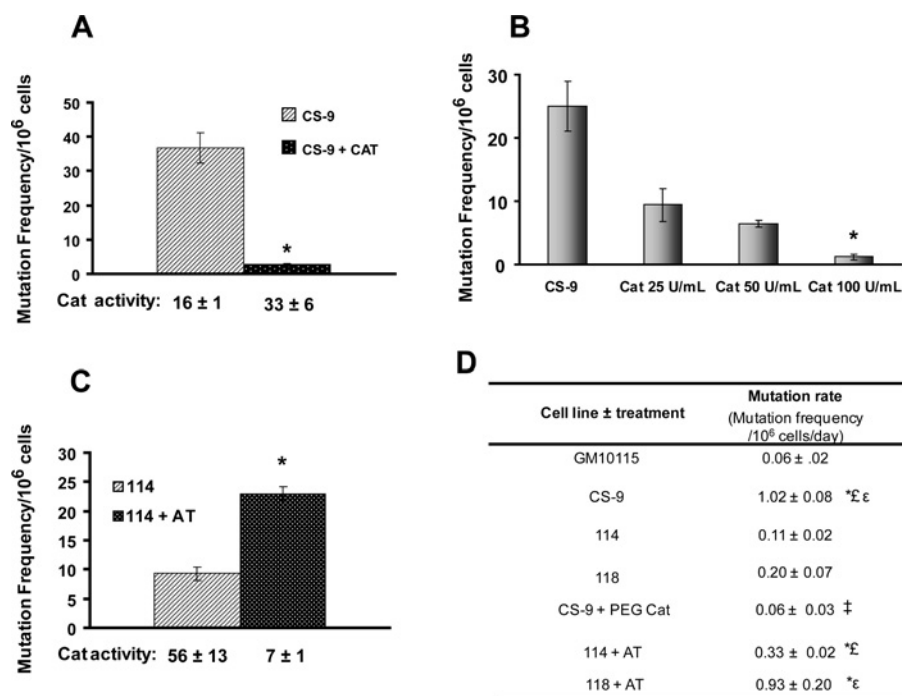


**Figure 4**  $H_2O_2$  causes radiation-induced delayed mutagenesis

(A) PEG-CAT (100 units/ml) was added to the CS-9 clone cells 2 h prior to the addition of 6-thioguanine during the mutation frequency assay and left for 2 weeks. The results represent  $\pm 1$  S.D. from four samples.  $*P < 0.001$  against clone CS-9 alone. (B) The suppressive effect that PEG-CAT had on mutation frequency in CS-9 was dose-dependent. The results represent the average of two samples in the 25 units/ml as well as the 50 units/ml group and four samples for the CS-9 as well as the 100 units/ml group.  $*P < 0.001$  against the clone CS-9 alone. (C) The stable clone 114 was grown in presence of AT for 4 days. On the fourth day, treated cells were plated in presence of 6-thioguanine for the mutation frequency assay. The error bars represent  $\pm 1$  S.D. from three experiments.  $*P < 0.01$  against clone 114. (D) The mutation rate in stable and unstable cells with or without manipulation of catalase activity was determined following selection in HAT media. The rates represent mutation frequency/ $10^6$  cells per day. Each data set represents the average of three separate dishes.  $P < 0.05$ ; \*against GM10115, ‡against CS-9, £against clone 114, εagainst clone 118.

greater increase in peroxide levels following AT treatment (results not shown). These results clearly show that radiation-induced genomic instability is a dynamic process that can be manipulated for many generations following radiation exposure by altering the activity of the specific  $\text{H}_2\text{O}_2$  scavenging enzyme catalase.

## DISCUSSION

Several theories have been proposed to explain the trans-generational nature of radiation-induced mutator phenotypes, with the ‘‘DNA repair hypothesis’’ being one of the most prominent [1,20]. According to this theory, a mutator phenotype can arise if exposure to radiation damages a critical gene coding for a protein that plays a role in DNA repair. In such a case, it is thought that cells would continue to show increased mutagenesis that would persist as a trans-generational phenotype. While some evidence in favour of this theory has accumulated [21], the small ‘target size’ presented by the genes encoding repair proteins, coupled with uncertainty surrounding the underlying source of spontaneous DNA damage, make it unlikely that repair genes are the only targets for radiation-induced mutator phenotypes (reviewed in [22]). Further support for this idea comes from past work showing the frequency of ionizing radiation-induced genomic instability in any surviving clone to be  $\sim 3\%$  per Gy [23], an incidence far too high to be explained by single (or even multiple) hit theories. It has also been shown by a rigorous microarray analysis that even though the genes associated with various signalling pathways are differentially down-regulated in the unstable clones, no single signalling pathway or repair gene correlated with a particular end-point of genomic instability [24].

Since genomic instability has also been associated with metabolic oxidative stress, a possible additional target for ionizing radiation-induced genomic instability could be genes coding for proteins involved in metabolic processes capable of producing ROS [3,6,22,25,26]. This hypothesis is supported by the fact that the progeny of irradiated cells show some evidence of dysfunctional mitochondria [6] and oxidative stress [4,6,7]. In addition, it was reported that pretreatment with free radical scavengers is capable of inhibiting the occurrence of radiation-induced genomic instability [27]. However, until now, studies identifying the specific ROS that cause persistent trans-generational radiation-induced mutator phenotypes were lacking.

The present study focused on identifying the role of  $\text{O}_2^{\bullet-}$  and  $\text{H}_2\text{O}_2$  in the mechanism of radiation-induced genomic instability. The results showed no consistent changes in the steady-state levels of  $\text{O}_2^{\bullet-}$  or the superoxide-scavenging enzymes, CuZnSOD and MnSOD, in unstable or stable clones. In contrast, radiation-induced genomically unstable cell lines demonstrated significantly increased steady-state levels of  $\text{H}_2\text{O}_2$ . Analysis of genomically stable cell lines did, however, show a significant increase in the  $\text{H}_2\text{O}_2$ -scavenging enzymes GPx and catalase. When the unstable cells were treated with a cell-permeant specific scavenger of  $\text{H}_2\text{O}_2$ , PEG-CAT, mutation frequency and mutation rates were dramatically suppressed. In addition, when catalase activity was inhibited in stable clones, mutation frequency and mutation rates were significantly increased. These results conclusively identify  $\text{H}_2\text{O}_2$  as the primary cause of the radiation-induced mutator phenotype in this model system.

The identification of intracellular  $\text{H}_2\text{O}_2$  as being causally involved with radiation-induced trans-generational genomic instability provides a mechanistic backdrop for the mutator phenotype hypothesis and suggests the critical importance of oxidative metabolic processes [7,20]. The central dogma in mammalian cell biology is that genetic material (DNA) undergoes transcription

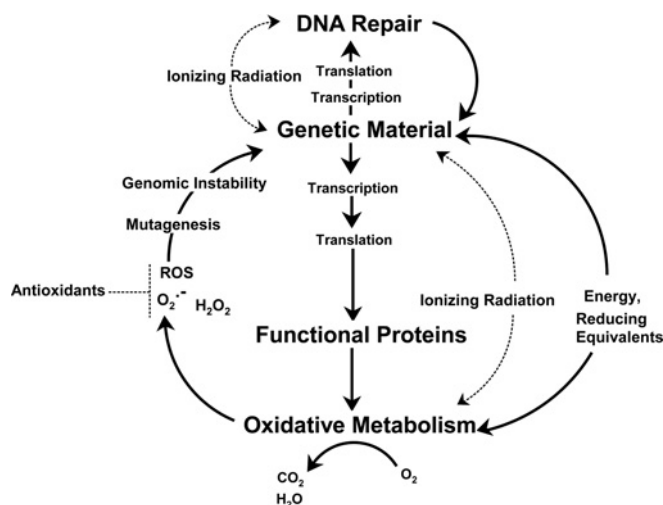


**Figure 5** Incorporation of oxidative metabolism into the mutator phenotype hypothesis

A cell signalling pathway where oxidative metabolism can be incorporated into the mutator phenotype hypothesis to explain the progression of radiation-induced genomic instability.

and translation to make functional proteins that execute essential cellular processes (i.e. production of energy and reducing equivalents necessary for metabolism and biosynthesis). In Figure 5, we show a theoretical model by which oxidative metabolism leading to the production of  $\text{H}_2\text{O}_2$  can be incorporated into the mutator phenotype hypothesis. In this model, radiation can damage genes coding for proteins involved in either oxidative metabolism or DNA repair. When radiation damages genes coding for proteins capable of resulting in increased levels of  $\text{H}_2\text{O}_2$ , a heritable change in steady-state levels of pro-oxidants leading to metabolic oxidative stress could occur. The resulting pro-oxidant intracellular environment could then perpetuate the process of mutagenesis, leading to genomic instability. Additional perturbation to the redox homeostasis in cells could increase stress-induced damage to genes coding for DNA repair and further exacerbate genomic instability [20,21,28]. This model would predict a feed-forward loop where radiation-induced metabolic oxidative stress in concert with damage to DNA repair machinery could progressively accelerate genomic destabilization, leading to the plethora of deleterious biological effects associated with late radiation damage. This model also significantly increases the effective target size for heritable damage capable of leading to genomic instability, which is consistent with the prevalence and variety of unstable phenotypes that have been observed following radiation.

The model in Figure 5 also predicts that cellular and dietary antioxidants specifically directed at mitigating the effects of hydroperoxides could rescue mammalian cells from this fate, effectively breaking the feed-forward loop and thereby slowing the progression of the radiation-induced mutator phenotype. Antioxidants can slow the rate of oxidative damage and might also allow for high-fidelity repair processes to work more effectively. The net result might be that, in the presence of antioxidants, high-fidelity repair capacity could offset the rate of damage, significantly reducing the progression of unstable phenotypes. Since genomic instability is thought to be an early step in tumorigenesis as well as degenerative diseases associated with aging, using specific scavengers of hydroperoxides to abrogate deleterious effects of radiation provides an attractive biochemical

rationale for the development of strategies to mitigate a broad range of radiation-induced effects.

This work is supported by the U.S. Department of Energy and NIH grants DE-FG02-05ER64050, RO1CA100045 and P30-CA086862. We thank Ling Li, Mitchell C. Coleman and Nükhet-Aykin Burns for discussions regarding the antioxidant enzyme assays, Kjerstin M. Owens for discussions related to the mutation rate assay and Melissa A. Fath for discussions regarding the EPR protocol and Ehab H. Sarsour for editorial assistance. We also thank the Flow Cytometry facility and the ESR facility at the University of Iowa.

## REFERENCES

- Morgan, W. F. (2003) Non-targeted and delayed effects of exposure to ionizing radiation: II. Radiation-induced genomic instability and bystander effects *in vivo*, clastogenic factors and transgenerational effects. *Radiat. Res.* **159**, 581–596
- Azzam, E. I., de Toledo, S. M., Spitz, D. R. and Little, J. B. (2002) Oxidative metabolism modulates signal transduction and micronucleus formation in bystander cells from  $\alpha$ -particle-irradiated normal human fibroblast cultures. *Cancer Res.* **62**, 5436–5442
- Hunt, C. R., Sim, J. E., Sullivan, S. J., Featherstone, T., Golden, W., Von Kapp-Herr, C., Hock, R. A., Gomez, R. A., Parsian, A. J. and Spitz, D. R. (1998) Genomic instability and catalase gene amplification induced by chronic exposure to oxidative stress. *Cancer Res.* **58**, 3986–3992
- Clutton, S. M., Townsend, K. M., Walker, C., Ansell, J. D. and Wright, E. G. (1996) Radiation-induced genomic instability and persisting oxidative stress in primary bone marrow cultures. *Carcinogenesis* **17**, 1633–1639
- Limoli, C. L. and Giedzinski, E. (2003) Induction of chromosomal instability by chronic oxidative stress. *Neoplasia* **5**, 339–346
- Limoli, C. L., Giedzinski, E., Morgan, W. F., Swartz, S. G., Jones, G. D. and Hyun, W. (2003) Persistent oxidative stress in chromosomally-unstable cells. *Cancer Res.* **63**, 3107–3111
- Kim, G. J., Fiskum, G. M. and Morgan, W. F. (2006) A role for mitochondrial dysfunction in perpetuating radiation-induced genomic instability. *Cancer Res.* **66**, 10377–10383
- Limoli, C. L., Kaplan, M. I., Corcoran, J. J., Meyers, M., Boothman, D. A. and Morgan, W. F. (1997) Chromosomal instability and its relationship to other end points of genomic instability. *Cancer Res.* **57**, 5557–5563
- Panus, P. C., Radi, R., Chumley, P. H., Lillard, R. H. and Freeman, B. A. (1993) Detection of H<sub>2</sub>O<sub>2</sub> release from vascular endothelial cells. *Free Radic. Biol. Med.* **14**, 217–223
- Kaschnitz, R. M., Hatefi, Y., Pedersen, P. L. and Morris, H. P. (1979) Isolation of mitochondria from Morris hepatomas. *Methods Enzymol.* **55**, 79–88
- Buettner, G. R. (1987) Spin trapping: ESR parameters of spin adducts. *Free Radic. Biol. Med.* **3**, 259–303
- Lawrence, R. A. and Burk, R. F. (1976) Glutathione peroxidase activity in selenium-deficient rat liver. *Biochem. Biophys. Res. Commun.* **71**, 952–958
- Lowry, O. H., Rosebrough, N. J., Farr, A. L. and Randall, R. J. (1951) Protein measurement with the Folin phenol reagent. *J. Biol. Chem.* **193**, 265–275
- Aebi, H. (1984) Catalase *in vitro*. *Methods Enzymol.* **105**, 121–126
- Anderson, M. E. (1985) *Handbook of Methods for Oxygen Radical Research*, CRC Press, Florida
- Griffith, O. W. (1980) Determination of glutathione and glutathione disulfide using glutathione reductase and 2-vinylpyridine. *Anal. Biochem.* **106**, 207–212
- Spitz, D. R. and Oberley, L. W. (1989) An assay for superoxide dismutase activity in mammalian tissue homogenates. *Anal. Biochem.* **179**, 8–18
- Glaab, W. E. and Tindall, K. R. (1997) Mutation rate at the hprt locus in human cancer cell lines with specific mismatch repair-gene defects. *Carcinogenesis* **18**, 1–8
- Li, S., Yan, T., Yang, J. Q., Oberley, T. D. and Oberley, L. W. (2000) The role of cellular glutathione peroxidase redox regulation in the suppression of tumor cell growth by manganese superoxide dismutase. *Cancer Res.* **60**, 3927–3939
- Loeb, L. A. (2001) A mutator phenotype in cancer. *Cancer Res.* **61**, 3230–3239
- Hinz, J. M., Tebbs, R. S., Wilson, P. F., Nham, P. B., Salazar, E. P., Nagasawa, H., Urbin, S. S., Bedford, J. S. and Thompson, L. H. (2006) Repression of mutagenesis by Rad51D-mediated homologous recombination. *Nucleic Acid Res.* **34**, 1358–1368
- Spitz, D. R., Azzam, E. I., Li, J. J. and Gius, D. (2004) Metabolic oxidation/reduction reactions and cellular responses to ionizing radiation: a unifying concept in stress response biology. *Cancer Metastasis Rev.* **23**, 311–322
- Limoli, C. L., Corcoran, J. J., Milligan, J. R., Ward, J. F. and Morgan, W. F. (1999) Critical target and dose and dose-rate responses for the induction of chromosomal instability by ionizing radiation. *Radiat. Res.* **151**, 677–685
- Snyder, A. R. and Morgan, W. F. (2005) Lack of consensus gene expression changes associated with radiation-induced chromosomal instability. *DNA Repair* **4**, 958–970
- Huang, L., Snyder, A. R. and Morgan, W. F. (2003) Radiation-induced genomic instability and its implications for radiation carcinogenesis. *Oncogene* **22**, 5848–5854
- Slane, B. G., Aykin-Burns, N., Smith, B. J., Kalen, A. L., Goswami, P. C., Domann, F. E. and Spitz, D. R. (2006) Mutation of succinate dehydrogenase subunit C results in increased O<sub>2</sub><sup>•-</sup>, oxidative stress, and genomic instability. *Cancer Res.* **66**, 7615–7620
- Limoli, C. L., Kaplan, M. I., Giedzinski, E. and Morgan, W. F. (2001) Attenuation of radiation-induced genomic instability by free radical scavengers and cellular proliferation. *Free Radic. Biol. Med.* **31**, 10–19
- Mondello, C., Rebuzzini, P., Dolzan, M., Edmonson, S., Taccioli, G. E. and Giulotto, E. (2001) Increased gene amplification in immortal rodent cells deficient for the DNA-dependent protein kinase catalytic subunit. *Cancer Res.* **61**, 4520–4525

Received 6 December 2007/7 March 2008; accepted 19 March 2008

Published as BJ Immediate Publication 19 March 2008, doi:10.1042/BJ20071643